Materials Today Bio 23 (2023) 100841

Contents lists available at ScienceDirect

Materials Today Bio

journal homepage: www.journals.elsevier.com/materials-today-bio

Construction of a novel cell-free tracheal scaffold promoting vascularization for repairing tracheal defects

Zhiming Shen [a,b,c], Fei Sun [d,a,b,c], Yibo Shan [a,b,c], Yi Lu [a,b,c], Cong Wu [a,b,c], Boyou Zhang [e], Qiang Wu [e], Lei Yuan [a,b,c], Jianwei Zhu [a,b,c], Qi Wang [a,b,c], Yilun Wang [a,b,c], Wenxuan Chen [a,b,c], Yaojing Zhang [a,b,c], Wenlong Yang [a,b,c], Yiwei Fan [a,b,c], Hongcan Shi [a,b,c,*]

[a] Clinical Medical College, Yangzhou University, Yangzhou, China
[b] Institute of Translational Medicine, Medical College, Yangzhou University, Yangzhou, China
[c] Jiangsu Key Laboratory of Integrated Traditional Chinese and Western Medicine for Prevention and Treatment of Senile Diseases, Yangzhou University, Yangzhou, China
[d] Taizhou People's Hospital, The Department of Thoracic Surgery, 225399, China
[e] The Second Xiangya Hospital, Central South University, Changsha, 410011, China

ARTICLE INFO

Keywords:
Endothelial progenitor cell
Exosomes
Trachea
Microvascularization

ABSTRACT

Functional vascularization is crucial for maintaining the long-term patency of tissue-engineered trachea and repairing defective trachea. Herein, we report the construction and evaluation of a novel cell-free tissue-engineered tracheal scaffold that effectively promotes vascularization of the graft. Our findings demonstrated that exosomes derived from endothelial progenitor cells (EPC-Exos) enhance the proliferation, migration, and tube formation of endothelial cells. Taking advantage of the angiogenic properties of EPC-Exos, we utilized methacrylate gelatin (GelMA) as a carrier for endothelial progenitor cell exosomes and encapsulated them within a 3D-printed polycaprolactone (PCL) scaffold to fabricate a composite tracheal scaffold. The results demonstrated the excellent angiogenic potential of the methacrylate gelatin/vascular endothelial progenitor cell exosome/polycaprolactone tracheal scaffold. Furthermore, in vivo reconstruction of tracheal defects revealed the capacity of this composite tracheal stent to remodel vasculature. In conclusion, we have successfully developed a novel tracheal stent composed of methacrylate gelatin/vascular endothelial progenitor exosome/polycaprolactone, which effectively promotes angiogenesis for tracheal repair, thereby offering significant prospects for clinical and translational medicine.

1. Introduction

Tracheal transplantation remains an unresolved clinical challenge worldwide. This is primarily due to the unique structure and function of the trachea [1]. Long-segment tracheal pathologies caused by tracheal tumors, stenosis, trauma, and softening (affecting over 50 % of adults or 30 % of children) contribute to increased surgical complications, while ensuring long-term viability and functionality of transplanted tracheal tissue poses further hurdles [2,3]. Therefore, tracheal reconstruction remains a pressing issue in current clinical practice. Mature vascular network can effectively promote the exchange of nutrients and metabolites between blood and tissue, and is an important part of biological tissue [4]. Thus, a tissue-engineered trachea needs to form a similar microvascular tissue. However, the arteriolar microvascular network in the trachea is mainly derived from the right inferior thyroid artery and bronchial artery, so it lacks good vascular supply, which becomes the main challenge of obtaining adequate vascular support for bioengineered trachea [5,6]. Tracheal vascularization is very important to prevent graft necrosis, promote tissue growth, assist innervation and improve graft activity [7,8]. Vascularization also plays a key role in promoting the growth of living mucous membranes to ensure adequate clearance of mucinous cilia [9].

Endothelial progenitor cells (EPCs) are the precursors of vascular endothelial cells, which are immature endothelial cells with migration characteristics and can further proliferate and differentiate [10–12]. It is main function that to participate in the vasculogenesis of ischemic tissue and repair of vascular injury after birth [13]. However, recent studies suggest that stimulation of adjacent intact endothelial cells through

* Corresponding author. Clinical Medical College, Yangzhou University, Yangzhou, China.
E-mail address: Shihongcan@yzu.edu.cn (H. Shi).

https://doi.org/10.1016/j.mtbio.2023.100841
Received 6 June 2023; Received in revised form 26 September 2023; Accepted 19 October 2023
Available online 20 October 2023
2590-0064/© 2023 Published by Elsevier Ltd. This is an open access article under the CC BY-NC-ND license (http://creativecommons.org/licenses/by-nc-nd/4.0/).

paracrine mechanisms may be more important for vascular repair than direct incorporation and expansion of exogenous transplanted EPCs during tissue repair [14]. Exosomes are small membrane particles (30–200 nm in diameter) from multivesicular bodies (MVBs), which are important components of paracrine [15]. As intercellular messengers, exosomes can transport important functional substances of cells into cells and regulate specific functions of target cells [16]. It has been reported that exobodies exhibit similar functional properties to their source cells without significant side effects such as ethics, immune rejection, malignant transformation and vascular obstruction, suggesting that exosome therapy is a safer and more promising tissue regeneration therapy than using cells directly [17,18]. In addition, exosomes are able to be transmitted between species without eliciting an obvious immune response, providing great advantages for direct use of exosomes [19]. Therefore, it could be speculated that exosomes derived from EPCs (EPC-Exos) trigger angiogenesis, and exosomes are released from cells and taken up by endothelial cells under interaction, promoting the survival and proliferation of endothelial cells in capillary-like structures, and promoting angiogenesis.

GelMA is obtained by reacting gelatin with methacrylic anhydride (MA). The large number of amino groups in the side chain of the gelatin are replaced by the methyl acryyl group in the methacrylic anhydride to form the modified gelatin [20–22]. However, the temperature - induced solid-liquid conversion of this modified gelatin is similar to that of gelatin. The modified gelatin has the properties of photocrosslinking due to the presence of methyl acrylyl group. After the addition of the photoinitiator, the GelMA hydrogel with good thermal stability was formed by crosslinking the aqueous solution of the modified gelatin under the light [23]. The GelMA hydrogel retains RGD and MMP sequences, which is still able to support cellular behavior without compromising the biocompatibility and degradation of gelatin [24,25]. In addition, the physical and chemical properties of GelMA hydrogel can be flexibly adjusted to meet the requirements of a variety of applications [26]. In recent years, polycaprolactone (PCL) has been gradually used in tissue engineering due to its excellent mechanical properties and biocompatibility. Ghorbani et al. implanted the PCL scaffold then planted adipose stem cells and chondrocytes to construct the tissue-engineered trachea [27]. The results proved that the PCL scaffold had good biocompatibility and appropriate mechanical properties.

The study creatively combined the advantages of GelMA hydrogel, vascular endothelial progenitor cell exosome and polycaprolactone. GelMA hydrogel was used to load exosomes and wrap PCL scaffolds to construct composite tracheal scaffolds. The scaffold can promote the migration of vascular endothelial cells in the defect area, Exosomes released by scaffolds can be internalized by vascular endothelial cells to promote the proliferation of vascular endothelial cells, thus promoting the repair and regeneration of trachea.

2. Methods

2.1. Animal care and ethics statement

All animal experiments in the study were approved by the Ethics Committee of yangzhou University School of Medicine (202207002).

2.2. Extraction and identification of EPCs

The isolation and culture of EPCs were conducted using whole marrow differential adherence. Briefly, bone marrow was isolated from the femurs of 3-week-old female rabbits and cultured in DMEM-F12 medium containing 10 % fetal bovine serum (FBS, Gibco, NY, USA) in an incubator (HERAcell 150i, Thermo Fisher, Waltham, USA) at 37 °C in 5 % CO2 for 20 h. Nonadherent cells were then collected and cultured in EBM-2MV medium (Lonza, Basel, Switzerland). Subsequently, the medium was replaced every two days [28]. The EPCs were harvested at the second passage (P2) and stained with the following fluorescence-conjugated antibodies: CD31 (Bioss, Beijing, China), CD34 (Genetex, SC, USA), CD45 (Bioss, Beijing, China), and CD 133 (Bioss, Beijing, China). The EPCs were also analyzed by immunofluorescence (IF) staining with FITC-UEA-l and Dil-ac-LDL.

2.3. Exosome isolation

When the EPCs were cultured to a degree of fusion of about 70 %–80 %, the culture was continued in serum-free EBM-2 medium for 24–40 h. Conditional media were collected and the number of cell lines was counted. The collected culture medium was first centrifuged at 2000×*g* (Beckman Coulter) for 20 min to remove cell debris, then collected by differential centrifugation at 10000×*g* for 30 min and 100000×*g* for 120 min. Re-suspended with 15 mL PBS, filtered with a 0.22 μm filter (microporous), and centrifuged at 4000×*g* to 200 μL.

2.4. Characterization of exosomes

Dynamic light scattering (DLS) analysis was performed using nanometer ™ technology (Malvern Instrument, Malvern, UK) to measure exosome size distribution. The size of exosomes was then analyzed using Zetasizer (Malvern) software. Transmission electron microscopy (TEM; HT7800; Hitachi, Tokyo, Japan) for exosome morphological observation. The total protein of EPC-exos was extracted and exosome surface markers CD9, CD63 and TSG101 were detected by Western blot.

2.5. Extraction and culture of vascular endothelial cells

The thoracic aortas of 4-week-old rabbits were dissected following standard surgical procedures. The aortas were clamped and the lumen was torn using forceps. Subsequently, they were immersed in 0.1 % type I collagenase and incubated at 37 °C for 2 h. The enzymatic solution was filtered through a 200-mesh filter and centrifuged at 1000 rpm for 5 min at room temperature. The obtained cells were resuspended in endothelial cell culture medium (ScienCell, San Diego, California, USA) supplemented with 5 % FBS, 1 % endothelial cell growth supplement (ECGS, ScienCell, San Diego, California, USA), and 1 % P/S. And then the samples were cultured for 48 h, and non-adherent cells were removed. Subsequently, the culture medium was changed every two days. Endothelial cells harvested at passage 2 (P2) were used for subsequent experiments.

2.6. Labeling of exosomes and internalization of exosomes by vascular endothelial cells

EPCs was labeled with a fluorescent lipophilic tracer Vybrant DiO (green) dye (molecular probe, Beyotime Biotechnology, China). EPCs were digested with trypsin and then resuspended in 1 mL medium. After adding 5 μL DiO solution, for suspension, the mixture was incubated in 5 % humidified carbon dioxide for 15min. After the mixture was centrifuged at 300×*g* for 10min and washed, the cells were cultured in complete medium to 50–60 % fusion. The exosomes were incubated with endothelial cells for 6 h after using the method described above to isolate EPC-Exos. After washing with PBS for 3 times, the endothelium was fixed with formalin for 15min. Vascular endothelial cells were then stained with DAPI for 5min. Finally, the samples were imaged using a fluorescence microscope (EVOS FL; Invitrogen, USA)) and confocal microscope (LSM 880NLO; CARL ZEISS, Germany).

2.6.1. Scanning electron microscopy (SEM)

The sample was fixed with 2.5 %(v/v) glutaraldehyde (Aladdin, Shanghai, China) in 0.1 m phosphate buffer (pH7.4) for 24 h. After rinsing in phosphate buffer, the material was dehydrated in graded ethanol, dried in a vacuum freeze dryer (LGJ-25C, SIF, China) at −48°Cfor 24 h, gilded by sputtering sublimation sputtering (ion sputtering coating instrument SCD500, BAL-TAL, USA), and scanned

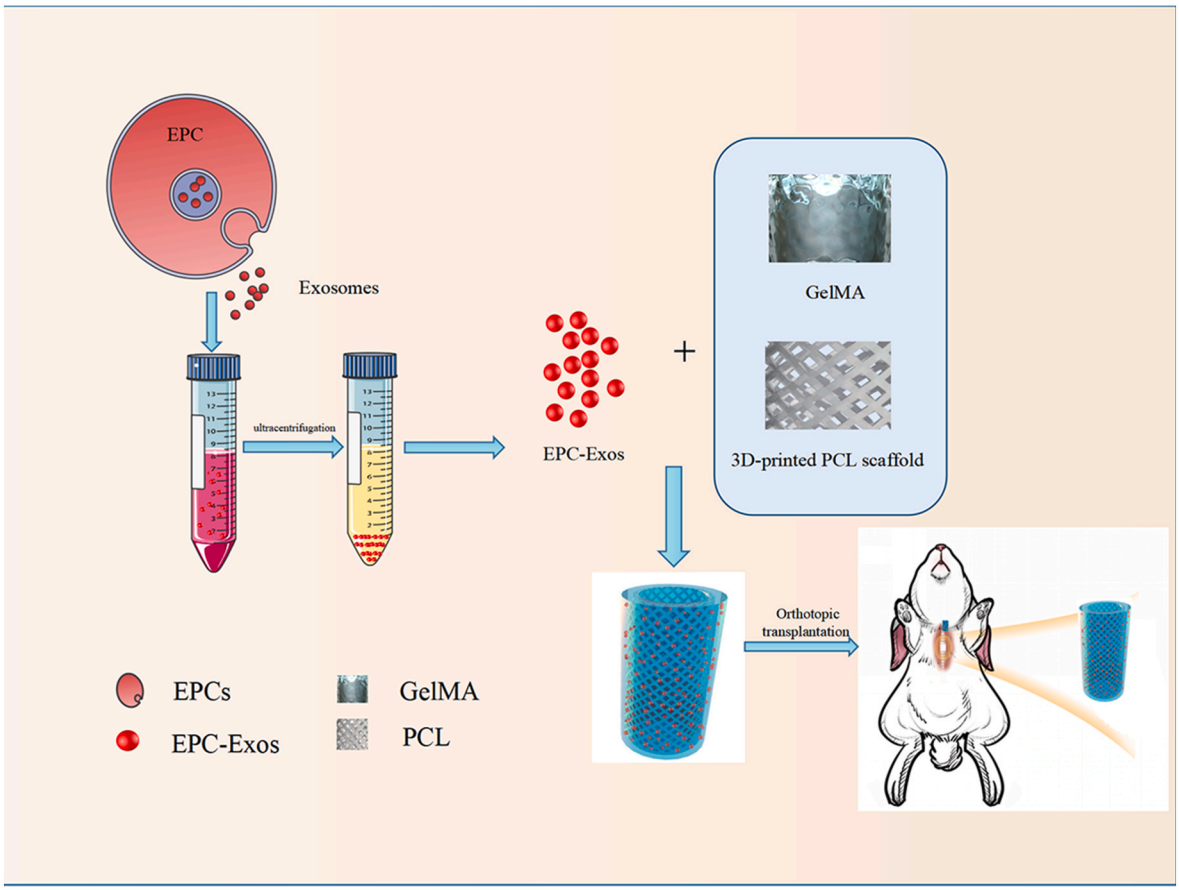

Fig. 1. Process diagram for constructing tracheal scaffold loaded with exosomes derived from endothelial progenitor cells.

electron microscopy (SEM; S-4800, Hitachi, Japan) observation.

2.7. Histological assessment

Tracheal scaffolds in each group were fixed in 4 % paraformaldehyde solution for 24 h, dehydrated in graded concentration of alcohol (100 %、95 %、80%和75 %), embedded in paraffin, and finally cut into 4 mm thickness. Sections were stained with hematoxylin and eosin (H&E) (Sorabio, China) and Masson's tricolor (MT) (Sorabio, China) according to the standard protocol. Staining sections were observed and collected using an optical microscope (Olympus, Japan).

2.8. Living/dead cell staining

For the staining of viable and dead cells using calcein-AM/propidium iodide (AM/PI, KeyGen Biotech, Jiangsu, China), cells were cultured in different concentrations of GelMA. After 48 h of incubation, the cells were stained with an AM/PI mixture and observed under an inverted fluorescence microscope.

2.9. Cell proliferation assay

Cell proliferation of endothelial cells in different groups was assessed using the Cell Counting Kit-8 (CCK-8, Biosharp, Hefei, China) after 1, 3, 5, and 7 days of culture.

2.10. Immunofluorescence (IF) analysis

The sections were first de-affinioned and rehydrated, then incubated with 0.4 % pepsin (Solarbio, Beijing, China) at 37 °C for 90min to repair the antigen. The slides were washed in distilled water and incubated in 5%BSA at 37 °C for 30min. They were then incubated overnight with CD31 antibody (GTX34489, Genetex, USA) or α-SMA antibody (GB13044, Servicebio, China) at 4°Cat a concentration of 1:200 overnight. Then, slices were incubated with the fluorescent secondary antibodies in 5%BSA at 37 °C in the dark at 1:500 for 60min. And then they were stained with DAPI (Beyotime, China) for 3min. The sections were rinsed with PBS and the images were taken with immunofluorescence microscopy.

2.11. Transwell assay

Cell suspension (100 μL) was added to the upper chamber of the Transwell inserts. In the lower chamber of a 24-well plate, 700 μL of culture medium was added. Exosomes were added to each group in the upper chamber. The cells were cultured for 12 h. After removing the Transwell inserts, they were lightly stained in 0.5 % crystal violet solution for 1 min. The migration of cells was observed under a microscope.

2.12. Preparation of composite scaffolds

We used biological 3D printing system (Regenovo 3D Bio-Architect®Sparrow) to print the stent. The printing nozzle is located on the rotation axis with the printing temperature of 90 °C. And the rotation axis rotates with the printing nozzle moving back and forth along the rotation axis at the printing speed of 3 mm/s. The Angle between the axis of each layer and the PCL fiber is 45°, forming a porous layer structure of 1 cm. The prepared GelMA was subjected to freeze-drying for preservation. Then GelMA was added to PBS with 0.25 % (w/v) lithium acylphosphinate photo-initiator (LAP) at different concentration of 10 %, 15 %, 20 % (w/v). The extracted exosomes were then added to

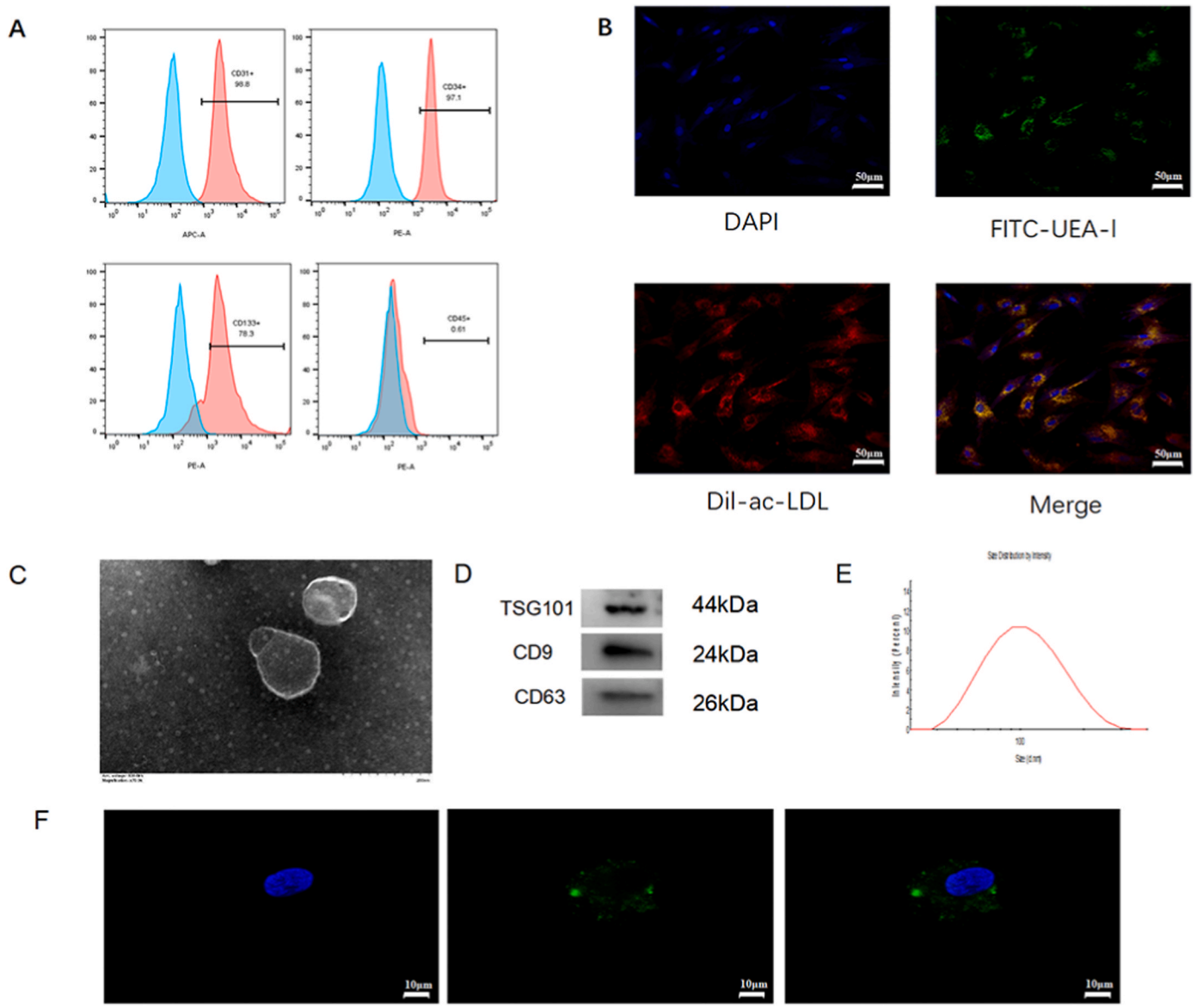

Fig. 2. Identification of endothelial progenitor cells and exosomes derived from endothelial progenitor cells. (A) Flow cytometry was employed to analyze the expression of CD31, CD34, CD133, and CD45 in EPCs. The blue histogram corresponds to cells without fluorescence antibody staining, while the red histogram represents cells stained with fluorescence antibodies. (B) EPCs were identified through specific fluorescence staining using FITC-UEA-l and Dil-ac-LDL. (C) The extracted exosomes were observed by transmission electron microscopy. (D) The marker proteins of exosomes, including TSG101, CD9, and CD63, were analyzed by Western blot to detect their expression. (E) The particle size of the exosome portion is about 100 nm in diameter. (F) Uptake of exosomes by endothelial cells. (For interpretation of the references to colour in this figure legend, the reader is referred to the Web version of this article.)

GelMA. GelMA loaded with exosomes was added to the PCL scaffold and the bio-ink was rapidly crosslinked under visible light. The irradiation intensity was 11 mW/cm^2 and lasted for 1min.

2.13. Mechanical performance testing of the scaffold

The length, outer diameter, and inner diameter of each sample were measured using a caliper. The biomechanical properties, including tensile strength, compressive performance, and three-point bending performance, were measured using an Autograph AGS-X series universal material testing machine (Shimadzu, Japan) [29,30].

2.14. Chicken chorioallantoic membrane (CAM) assays

The chorioallantoic membrane (CAM) assay was employed as an in vivo model to assess the angiogenesis characteristics of each group of tracheal grafts. Specific pathogen-free (SPF) fertilized eggs were incubated at a temperature of 37.8 °C with a humidity level of 55 %. On the 8th day of incubation, a window of approximately 2 cm in the eggshell was created using ophthalmic scissors and forceps after disinfection with 75 % alcohol. This allowed visualization of the embryo and CAM vessels. Subsequently, the chicken embryos were randomly divided into four groups: a negative control group with gelatin sponge (Johnson, NJ, USA) containing PBS (10 μL), experimental groups with PCL and PCL-GelMA-exos stents, and a positive control group with gelatin sponges containing VEGF (10 μL/1 μg, Petroleum Technology, NJ, USA). Each group's stents were trimmed to a size of approximately 2 × 2 × 1 mm^3 and placed in the avascular area between two anterior yolk veins near the embryo's head. The windows were sealed with medical tape, and the eggs were further incubated for an additional 3 days. The angiogenesis characteristics of the eggs were documented through daily photography. All procedures were conducted under aseptic conditions [31].

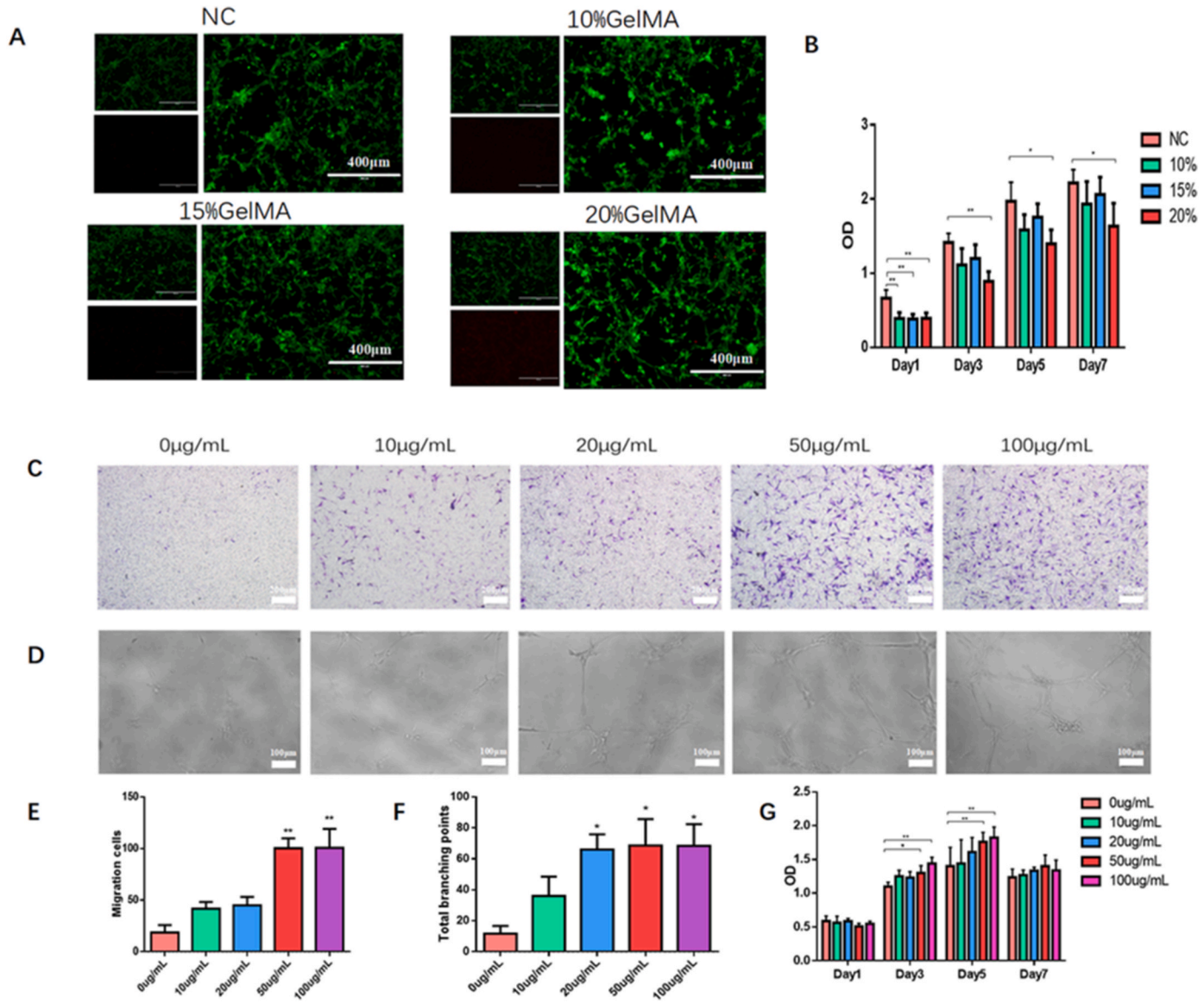

Fig. 3. GelMA and exosome concentration screening. (A) The influence of 10 %, 15 %, and 20 % GelMA concentrations on cell viability was assessed through Calcein-AM/PI staining. (B) CCK-8 assay revealed the optical density (OD) values of each group on days 1, 3, 5, and 7. (C) Transwell experiment assessed the effect of different exosome concentrations on cell migration. (D) The angiogenesis assay evaluated the impact of different exosome concentrations on endothelial cell vessel formation. (E) Quantification of migrated cells in the Transwell assay showed that 50 μg/mL and 100 μg/mL exosomes significantly promoted endothelial cell migration. (F) Statistical analysis of angiogenesis performance. (G) CCK-8 assay examined the influence of different exosome concentrations on cell proliferation, analyzing the OD values of each group on days 1, 3, 5, and 7. *$p < 0.05$; **$p < 0.01$.

2.15. Statistical analysis

Statistical analysis was performed using one-way analysis of variance (one-way ANOVA) or a two-tailed Student's t-test, utilizing GraphPad Prism 7 (San Diego, USA). Each experiment was replicated thrice, and the results are presented as mean ± standard deviation.

3. Results

3.1. Uptake of exosomes by vascular endothelial cells

The preparation process of the cell-free exosome-loaded composite scaffold is depicted in Fig. 1. First, we isolated endothelial progenitor cells (EPCs). The whole bone marrow differential adhesion method was used for the isolation and cultivation of EPCs. The results of flow cytometry and specific immunofluorescence staining indicated that EPCs were successfully extracted (Fig. 2A–B). EPCs were cultured in serum-free medium and exosomes were isolated from conditioned medium supernatant by supercentrifugation. Under transmission electron microscopy, exosomes show a typical cup-shaped shape with a diameter of about 100 nm (Fig. 2C). Dynamic light scattering (DLS) analysis was performed using nanometer ™ technology (Malvern Instrument, Malvern, UK) to measure size distribution of exosome ((Fig. 2E)). And the result also showed that the exosomes derived from EPCs were 50 nm–150 nm in diameter. Western blotting results showed that specific markers of exosome components CD9、CD63 and TSG101 were obtained (Fig. 2D). The labeled exosomes with DIO were observed around the nuclei of vascular endothelial cells after co-culture with exosomes for 6 h. The labeled EPC-Exos were observed around the nuclei of vascular endothelial cells (Fig. 2F), indicating that vascular endothelial cells could absorb components from EPC-Exos, indicating that vascular endothelial cells could absorb exosomal components from EPCs.

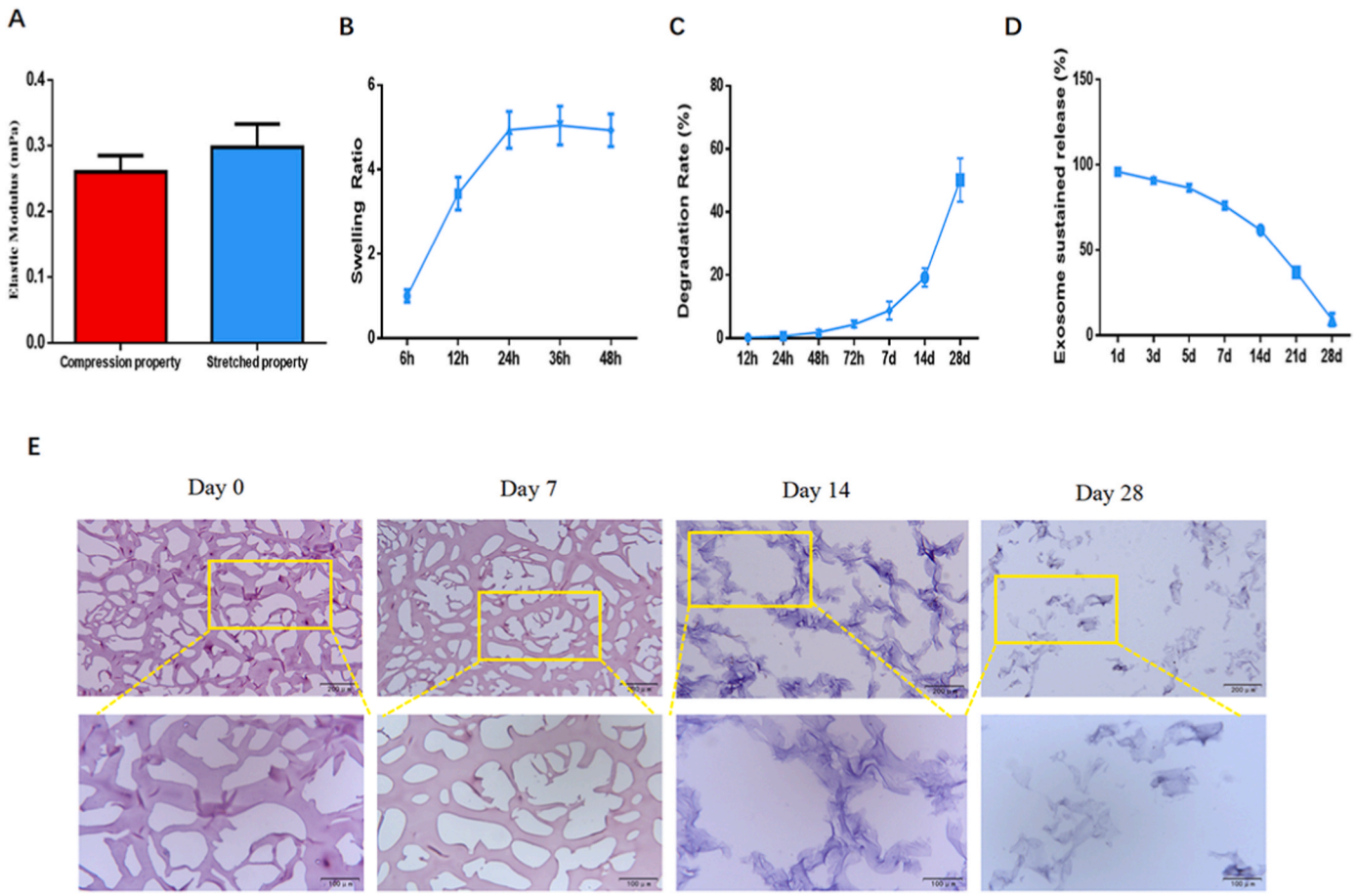

Fig. 4. Characterization of GelMA-Exos Hydrogels. (A) Compressive and Stretched testing revealed the mechanical properties of GelMA-Exos hydrogels. (B) Swelling ratios were quantified for GelMA-Exos hydrogels over time. (C) Degradation rates were determined for GelMA-Exos hydrogels at multiple time points post-fabrication. (D) Release kinetics of exosomes were profiled from GelMA-Exos hydrogels over 28 days. (E) H&E staining visualized the degradation process of GelMA-Exos hydrogels across distinct time points.

3.2. Effects of exosome and GelMA concentrations on vascular endothelial cells in vitro

When we cultured vascular endothelial cells, we added different concentrations of exosomes into the culture medium. The results showed that exosomes could promote the proliferation and migration of vascular endothelial cells when the concentration reached 50ug/mL (Fig. 3C–F). Interestingly, we found that extracellular vesicles at a concentration of 20ug/mL also promote angiogenesis (Fig. 3E), while 50ug/mL and 100ug/mL exosomes can promote the angiogenesis and migration of vascular endothelial cells (Fig. 3D–E). In addition, the CCK8 results also indicate that extracellular vesicles at a concentration of 50ug/mL promote the proliferation of endothelial cells (Fig. 3G). Therefore, the concentration of 50 μg/mL was chosen as the final concentration for the use of exosomes. Besides, Endothelial cells were cultured in GelMA at concentrations of 10 %, 15 %, and 20 %, respectively. The results of the live/dead cell experiments indicated that different concentrations of GelMA did not cause significant damage to the cells (Fig. 3A). However, the CCK8 assay results showed a significant decrease in cell proliferation in the 20 % GelMA concentration group compared to the control group (Fig. 3B). High concentration of GelMA was not conducive to the proliferation of vascular endothelial cells. Considering that the 15 % concentration of GelMA has better mechanical support properties compared to the 10 % concentration, the 15 % GelMA concentration was ultimately chosen as the concentration for scaffold preparation.

3.3. Preparations and characterization of hybrid scaffold

GelMA hydrogel serves as both a carrier and a delivery vehicle. We evaluated the mechanical properties, swelling, and degradation of GelMA-Exos (Fig. 4A–C). As a carrier for exosomes, we also monitored the release process of exosomes within GelMA over a 28-day period (Fig. 4D). Additionally, we applied H&E staining at various time intervals to observe the degradation process of GelMA(Fig. 4E). Although the mechanical properties of GelMA-Exos hydrogels were limited, they exhibited excellent swelling and degradation capacities. As a delivery vehicle, GelMA-Exos enabled sustained, localized release of bioactive exosomes to elicit therapeutic effects. As GelMA hydrogels exhibited limited mechanical properties, we sought a material with superior mechanics to serve as a scaffold. PCL has been widely used in regenerative medicine due to its excellent mechanical properties and biocompatibility. To extract the advantages of natural and synthetic materials, and further prevent tracheal collapse and improve the performance of the scaffold in promoting angiogenesis, we fabricated a 3D-printed polycaprolactone (PCL) scaffold as a supportive structure. The extracted EPC-Exos were loaded into GelMA to prepare GelMA-Exos hydrogels. GelMA was crosslinked and solidified onto PCL scaffolds under visible light at a wavelength of 405 nm, resulting in composite scaffolds loaded with exosomes. Macroscopic and microscopic structures of different scaffolds were observed using gross photography and scanning electron microscopy (SEM) (Fig. 5A and B), revealing that the PCL/GelMA scaffolds exhibited abundant microporous structures that were conducive to cell adhesion. The mechanical properties of the different scaffolds were

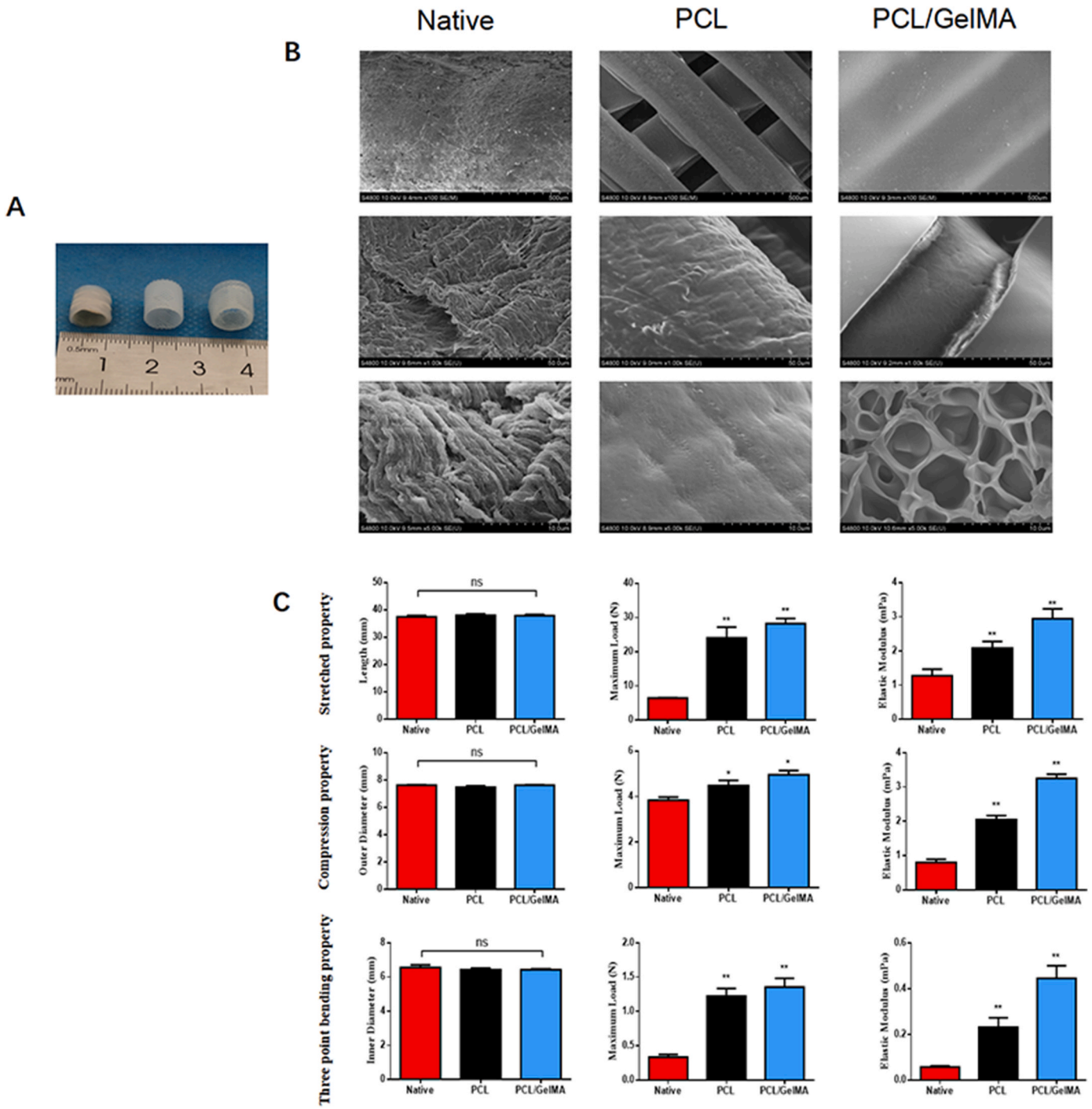

Fig. 5. Macroscopic and microscopic comparisons of different tracheal scaffolds, and their mechanical properties. (A) Macroscopic images of the native trachea, PCL scaffold, and PCL/GelMA scaffold. (B) Scanning electron microscopy images depict the comparative microstructures of different tracheal scaffolds. (C) Biomechanical performance testing of the native trachea, PCL scaffold, and PCL/GelMA scaffold, which was compared through tensile testing, compression testing, and three-point bending testing. *$p < 0.05$; **$p < 0.01$.

assessed using various mechanical testing methods. The results demonstrated that PCL/GelMA scaffolds exhibited excellent mechanical support, effectively preventing tracheal collapse after tracheal transplantation (Fig. 5C).

3.4. *In vivo angiogenic characteristics*

In vivo angiogenesis plays a crucial role in the functionalization of implants and long-term survival of transplant recipients. The effect of PCL/GelMA-Exos on promoting angiogenesis in vivo was evaluated using the chorioallantoic membrane (CAM) assay (Fig. 6A–B). Furthermore, hematoxylin and eosin (H&E) staining and CD31 immunohistochemistry (IHC) were conducted on identical areas to delineate the remaining scaffold and visualize infiltration by vasculature (Fig. 6C). In comparison to the PCL scaffold group, the PCL/GelMA-Exos group exhibited abundant microvascular growth surrounding and on the surface of the implants as early as 2 days after implantation, displaying a radial pattern of growth similar to the positive control group treated with angiogenic growth factors in GelMA sponges. And compared to the PCL group, the PCL/GelMA-Exos scaffold group exhibited significantly

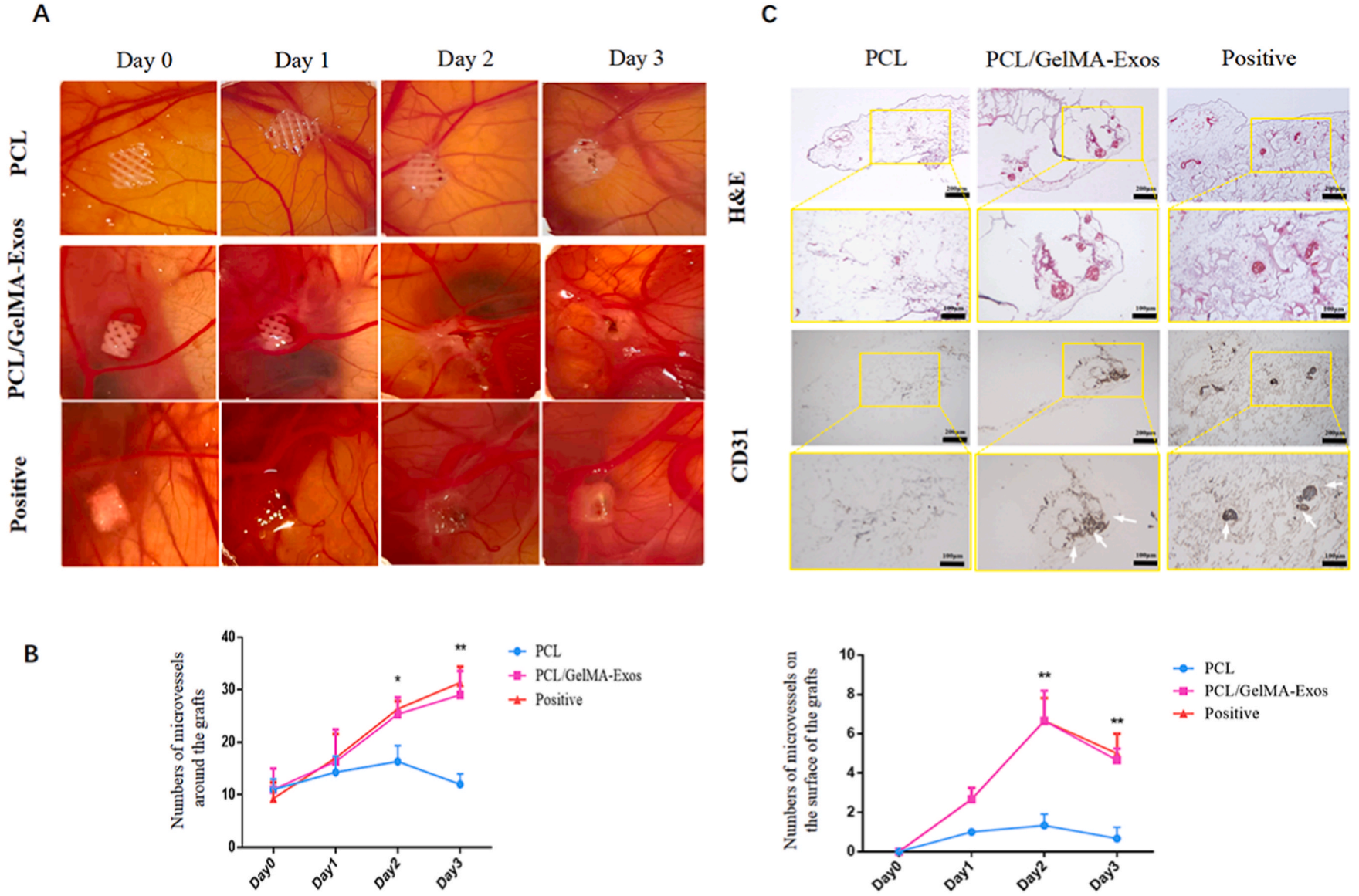

Fig. 6. The in vivo angiogenic performance of different scaffolds was assessed using the CAM assay. (A) CAM revealed the vascularization characteristics surrounding the implanted scaffolds (Positive, PCL, and PCL/GelMA-Exos groups) at 0, 1, 2, and 3 days. Compared to the PCL group, the PCL/GelMA-Exos group samples exhibited evident encapsulation by blood vessels from the urinary bladder, showing a radial distribution pattern. (B) Quantitative analysis of microvessel density on and surrounding the implants. (C) H&E staining and CD31 immunohistochemistry of matched areas to delineate residual scaffold and vascular infiltration. *$p < 0.05$; **$p < 0.01$.

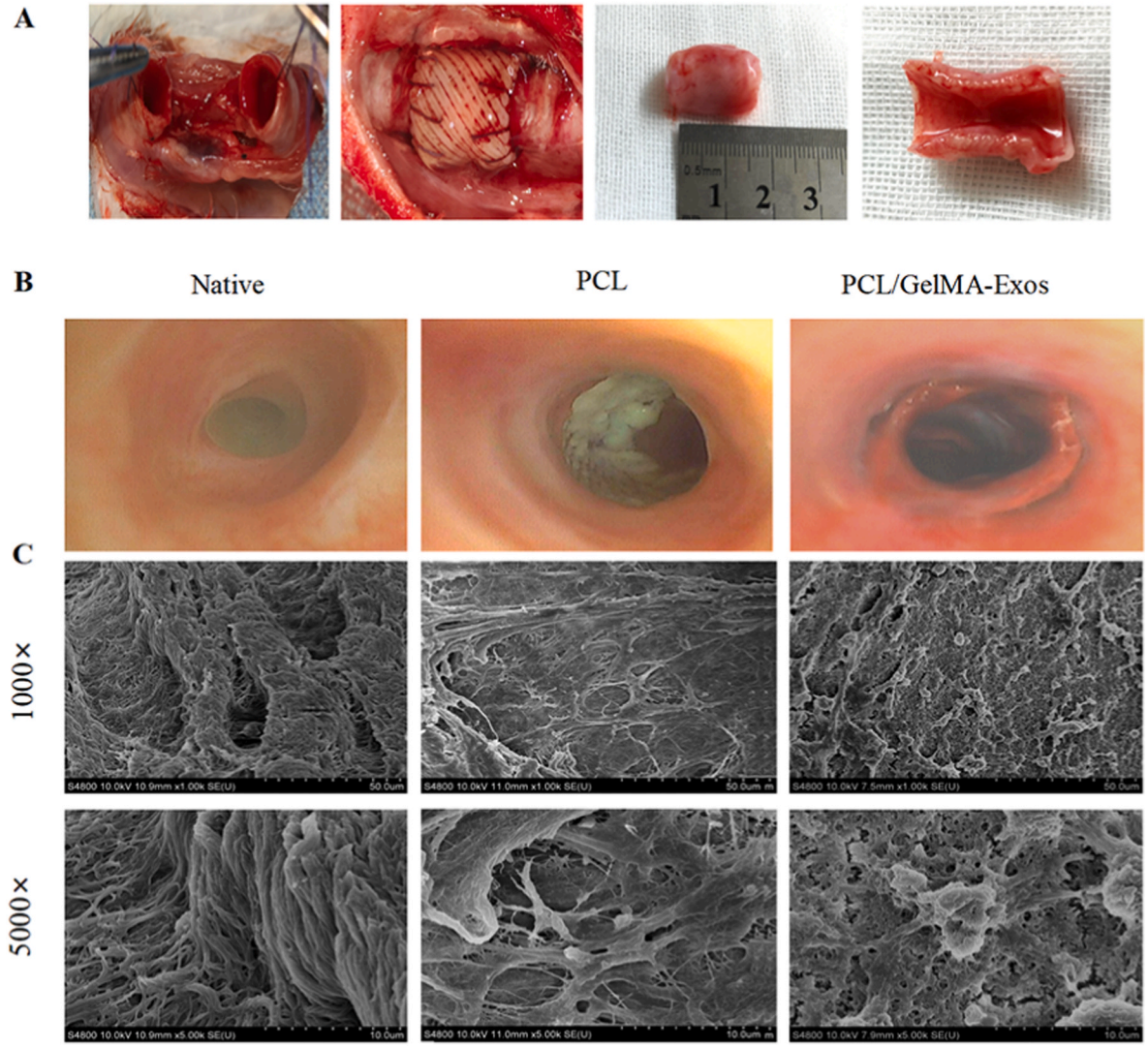

Fig. 7. Segmental tracheal reconstruction and postoperative examinations. (A) Surgical schematic diagram and macroscopic observation of postoperative specimens in the experimental group. (B) Tracheoscopic examination and macroscopic observation. (C) Scanning electron microscopy examination of the scaffolds in each group.

increased CD31 expression. These findings indicate that the PCL/GelMA-Exos scaffold effectively promotes vascular formation in vivo.

3.5. Studies on in situ transplantation

We conducted tracheal transplantation in a rabbit model with tracheal defects to further evaluate the preliminary application of bio-engineered in situ trachea in segmental tracheal reconstruction. The transplants were directly repaired using end-to-end anastomosis without ectopic embedding, to restore the segmental tracheal defect (Fig. 7A). Two months postoperatively, the luminal conditions of different scaffolds were examined via tracheoscopy. The PCL group exhibited a pale luminal color, lack of effective vascularization, and the presence of white mucus on the surface. In contrast, the PCL/GelMA-Exos group showed a bright red luminal wall with unobstructed passage, indicating vascular formation (Fig. 7B). Scanning electron microscopy results indicated greater cell adhesion and growth on the surface of the PCL/GelMA-Exos group compared to the PCL group, suggesting that the PCL/GelMA-Exos scaffold was more conducive to the growth and adhesion of tracheal tissue cells, facilitating tracheal repair and regeneration (Fig. 7C). Histological examination (H&E and MT staining) revealed a significant increase in microvascular formation at the graft site in the PCL/GelMA-Exos group compared to the PCL group (Fig. 8A). Furthermore, the expression of CD31 and α-SMA, markers of angiogenesis, was significantly elevated in the PCL/GelMA-Exos group (Fig. 8B–C). These findings indicate that PCL/GelMA-Exos effectively promotes microvascular formation in situ transplantation.

4. Discussion

Tissue engineering techniques provide significant opportunities for tracheal reconstruction surgery but also face several challenges, including the preparation of non-immunogenic tracheal grafts, maintaining favorable biomechanical properties of the grafts, and constructing vascularized structures [32–35]. These challenges are crucial factors determining the success of tracheal replacement therapies and long-term recipient survival. Vascularization of the scaffold is essential for restoring graft functionality and ensuring its survival in tissue-engineered tracheal transplantation. Vascularization provides sufficient oxygen and nutrients while removing waste products, thus meeting the metabolic demands and physiological functions of the graft [36]. Additionally, vascularization promotes the clearance of immune cells and inflammatory factors, contributing to a reduced risk of graft rejection and inflammation, ultimately improving graft survival and

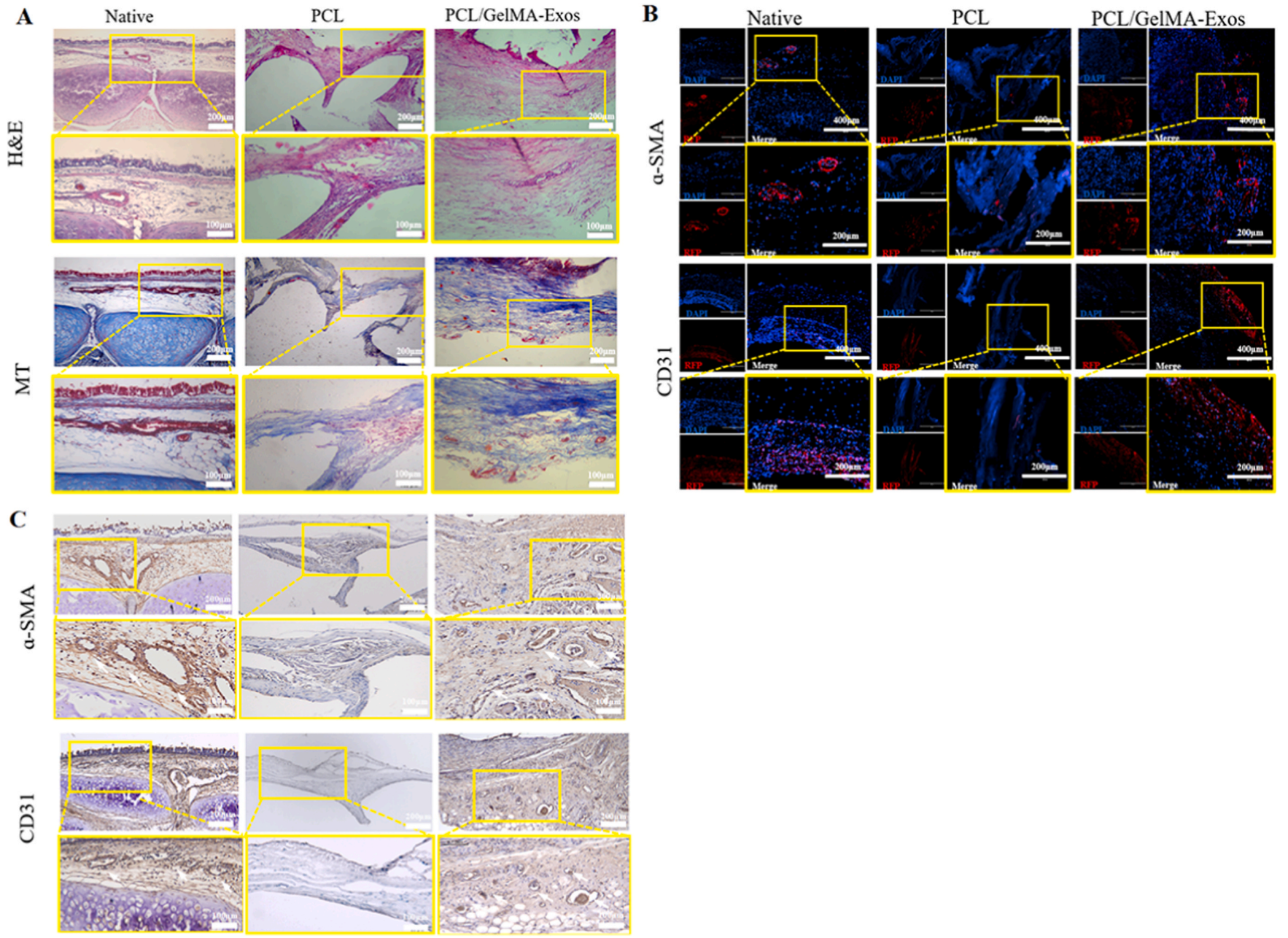

Fig. 8. Histological staining and immunofluorescence staining of 8-week post-transplantation tissues. (A) H&E and MT staining of each group, with red arrows indicating microvessels. (B) Immunofluorescence staining of α-SMA and CD31 in each group. (C) Immunohistochemical Staining for α-SMA and CD31 in each group. (For interpretation of the references to colour in this figure legend, the reader is referred to the Web version of this article.)

long-term survival rates [37]. Therefore, promoting complete vascularization of the graft is crucial in tissue-engineered tracheal transplantation. Cell seeding is one of the approaches employed in tissue engineering. However, direct cell transplantation entails various risks, including tumorigenicity, ethical concerns, immune rejection, and embolism [38–40]. Exosomes, as cell-to-cell messengers, facilitate the transport of important functional substances from donor cells to recipient cells and regulate specific functions of target cells through paracrine effects [41]. Therefore, utilizing exosomes allows harnessing the functionality of their parent cells while avoiding the risks associated with direct transplantation of cells. Moreover, exosomes can be transferred between different species without eliciting significant immune reactions. In this context, researchers have developed a novel cell-free tissue-engineered tracheal scaffold, circumventing concerns associated with tumorigenicity and ethical issues related to direct cell transplantation. This scaffold exhibits appropriate biomechanical properties and excellent biocompatibility, while effectively promoting vascular formation and restoring graft vascular supply, making it suitable for tissue-engineered tracheal transplantation.

Exosomes derived from endothelial progenitor cells (EPC-Exos) have been found to effectively promote endothelial cell proliferation and tube formation. We utilize the pro-angiogenic properties of EPC-Exos, along with the microporous structure and excellent biocompatibility of GelMA, as essential components of the composite scaffold. This combination effectively promotes cell growth and proliferation, facilitating microvascular formation and tissue repair. While pure GelMA exhibits good biocompatibility, it lacks sufficient mechanical properties to address issues of graft softening and collapse post-implantation. Therefore, we utilize 3D printing technology to fabricate PCL scaffolds that match the native trachea, incorporating GelMA loaded with EPC-Exos to construct a hybrid tracheal graft.

Our study compares the mechanical properties and pro-angiogenic performance of PCL scaffolds and PCL/GelMA-Exos scaffolds. Both in terms of mechanical properties and pro-angiogenic performance, the PCL/GelMA-Exos scaffold outperforms the PCL scaffold, resulting in superior outcomes post-transplantation compared to the PCL scaffold. EPC-Exos were found to be readily taken up by endothelial cells, significantly enhancing their angiogenic activity. This resulted in increased vascularization at the site of injury, as evidenced by elevated blood vessel density. Consequently, the process of tracheal repair was accelerated. Additionally, we screened the application concentration of GelMA. GelMA hydrogel is a biodegradable hydrogel material synthesized from gelatin and methacrylic acid (MA). It combines the advantages of gelatin and methacrylic acid, exhibiting excellent biocompatibility, tunability, degradability, and gel formation ability. In this study, we found that GelMA concentrations of 10 % and 15 % had no significant impact on endothelial cell proliferation and activity. Considering that 15 % GelMA exhibited superior mechanical support, and our scaffold required good mechanical properties, we ultimately selected 15 % GelMA as the scaffold material.

Currently, several primary strategies are utilized for vascularizing tracheal grafts. These include the ectopic wrapping method, wherein the graft is wrapped with omentum or mesentery prior to in situ transplantation and maintained for a few weeks; the utilization of decellularized trachea supplemented with preserved vascular growth factors to facilitate neovascularization; and the 3D bioprinting of vascularized grafts using a bioink incorporating bone marrow mesenchymal stem cells or endothelial cells. Although these approaches have demonstrated some degree of success in tracheal graft fabrication, they are not without limitations. The ectopic wrapping method may necessitate secondary surgery and is associated with significant trauma. Decellularized trachea may experience softening and collapse post-transplantation, requiring repeated implantation of tracheal stents. 3D bioprinted vascularized tissues exhibit relatively weak biomechanical properties, and the inclusion of cellular bioinks poses the risk of tumorigenesis and hyperplasia, thus failing to meet the performance requirements for long-segment tracheal grafts. Nevertheless, this study adopted an innovative one-step methodology to fabricate avascularized tracheal grafts, encompassing superior induction of vascularization and biomechanical properties. Additionally, the study introduced endothelial progenitor cell-derived exosomes (Exos) hydrogel as a novel approach to avoid the risk of tumorigenesis and hyperplasia associated with direct cell transplantation.

This study demonstrates promising progress in the development of tissue-engineered tracheal scaffolds utilizing exosome technology. The reported composite scaffold effectively promotes vascularization, which is key for long-term viability and integration of tracheal grafts. Looking ahead, research should focus on optimizing the scaffold design and exosome loading to enhance vascular remodeling. Thorough preclinical studies in animal models are needed to evaluate tracheal regeneration over extended periods. Safety and efficacy must be established before pursuing human clinical trials. If proven successful in humans, this cell-free, off-the-shelf tracheal scaffold could provide a practical alternative to autografts and allografts for tracheal reconstruction. The clinical merits of this approach include avoiding donor site morbidity and graft rejection, while supporting natural repair mechanisms through exosome signaling. For industry, the scaffold production process appears readily scalable. The polymers and exosomes could be mass-produced and assembled into patient-specific scaffolds using 3D printing. Standardized manufacturing paired with off-the-shelf availability would enable commercialization and widespread clinical adoption. As this technology matures, it may also be adaptable to other hollow organ systems with similar tissue engineering challenges. In summary, the researchers proposed a novel cell-free tissue-engineered tracheal scaffold that effectively promotes vascularization, thereby facilitating tracheal repair. The findings suggest that PCL/GelMA-Exos scaffolds hold promising potential as a strategy for rapid vascularization in tissue-engineered trachea and future clinical transplantation.

Credit author statement

Zhiming Shen, Fei Sun, Yibo Shan and Yi Lu contributed equally to this manuscript. Zhiming Shen, Fei Sun and Yibo Shan designed the whole study. Yi Lu completed the supplementary experiment. Yi Lu and Boyou Zhang finished in vivo experiments. Cong Wu and Qiang Wu supervised the experimental operation. Lei Yuan and Jianwei Zhu participated in vitro experiments. Qi Wang, Yilun Wang and Wenxuan Chen participated in animal surgery. Yaojing Zhang, Wenlong Yang and Yiwei Fan participated in revising the article. Hongcan Shi managed and guided the entire research project. All authors approved this manuscript.

Declaration of competing interest

The authors declare that they have no known competing financial interests or personal relationships that could have appeared to influence the work reported in this paper.

Data availability

Data will be made available on request.

Acknowledgements

The study was supported by the National Natural Science Foundation of China (No. 82070020), Postgraduate Research & Practice Innovation Program of Jiangsu Province (KYCX21_3287, KYCX 22_3567, SJCX22_1812) , Outstanding Doctoral Dissertation Fund of Yangzhou University and Yangzhou University Graduate International Academic Exchange Special Fund Project.

References

[1] B. Zhang, F. Sun, Y. Lu, Z. Wang, Z. Shen, L. Yuan, et al., A novel decellularized trachea preparation method for the rapid construction of a functional tissue engineered trachea to repair tracheal defects, J. Mater. Chem. B 10 (2022) 4810–4822, https://doi.org/10.1039/d1tb02100a.

[2] L. Soriano, T. Khalid, D. Whelan, N. O'Huallachain, K.C. Redmond, F.J. O'Brien, et al., Development and clinical translation of tubular constructs for tracheal tissue engineering: a review, Eur. Respir. Rev. 30 (2021), https://doi.org/10.1183/16000617.0154-2021.

[3] F. Sun, Y. Lu, Z. Wang, B. Zhang, Z. Shen, L. Yuan, et al., Directly construct microvascularization of tissue engineering trachea in orthotopic transplantation, Mater Sci Eng C Mater Biol Appl 128 (2021), 112201, https://doi.org/10.1016/j.msec.2021.112201.

[4] C.D. Roche, P. Sharma, A.W. Ashton, C. Jackson, M. Xue, C. Gentile, Printability, durability, contractility and vascular network formation in 3D bioprinted cardiac endothelial cells using alginate-gelatin hydrogels, Front. Bioeng. Biotechnol. 9 (2021), 636257, https://doi.org/10.3389/fbioe.2021.636257.

[5] E.M. Baile, The anatomy and physiology of the bronchial circulation, J. Aerosol Med. 9 (1996) 1–6, https://doi.org/10.1089/jam.1996.9.1.

[6] M.F. Sturridge, M.R. Mueller, T. Treasure, Blood supply of the trachea and proximal bronchi, Ann. Thorac. Surg. 84 (2007) 675, https://doi.org/10.1016/j.athoracsur.2007.01.007.

[7] Z. Shen, T. Xia, J. Zhao, S. Pan, Current status and future trends of reconstructing a vascularized tissue-engineered trachea, Connect. Tissue Res. (2023) 1–17, https://doi.org/10.1080/03008207.2023.2212052.

[8] J.A. Hardillo, P.V. Vander, P.R. Delaere, Transplantation of tracheal autografts: is a two-stage procedure necessary? Acta Oto-Rhino-Laryngol. Belg. 54 (2000) 13–21.

[9] F. Kreimendahl, S. Ossenbrink, M. Kopf, M. Westhofen, T. Schmitz-Rode, H. Fischer, et al., Combination of vascularization and cilia formation for three-dimensional airway tissue engineering, J. Biomed. Mater. Res. 107 (2019) 2053–2062, https://doi.org/10.1002/jbm.a.36718.

[10] J.X. Yang, Y.Y. Pan, X.X. Wang, Y.G. Qiu, W. Mao, Endothelial progenitor cells in age-related vascular remodeling, Cell Transplant. 27 (2018) 786–795, https://doi.org/10.1177/0963689718779345.

[11] M. Alwjwaj, R. Kadir, U. Bayraktutan, The secretome of endothelial progenitor cells: a potential therapeutic strategy for ischemic stroke, Neural Regen Res 16 (2021) 1483–1489, https://doi.org/10.4103/1673-5374.303012.

[12] O.A. Kolesnichenko, J.A. Whitsett, T.V. Kalin, V.V. Kalinichenko, Therapeutic potential of endothelial progenitor cells in pulmonary diseases, Am. J. Respir. Cell Mol. Biol. 65 (2021) 473–488, https://doi.org/10.1165/rcmb.2021-0152TR.

[13] E.B. Peters, Endothelial progenitor cells for the vascularization of engineered tissues, Tissue Eng., Part B 24 (2018) 1–24, https://doi.org/10.1089/ten.TEB.2017.0127.

[14] Y. Zha, Y. Li, T. Lin, J. Chen, S. Zhang, J. Wang, Progenitor cell-derived exosomes endowed with VEGF plasmids enhance osteogenic induction and vascular remodeling in large segmental bone defects, Theranostics 11 (2021) 397–409, https://doi.org/10.7150/thno.50741.

[15] G. Ambrosini, B. Ebert, R.D. Carvajal, G.K. Schwartz, A.J. Rai, Use of antibody arrays to probe exosome and extracellular vesicle mediated functional changes in cells, Methods Enzymol. 645 (2020) 43–53, https://doi.org/10.1016/bs.mie.2020.09.003.

[16] Y. Zhang, J. Bi, J. Huang, Y. Tang, S. Du, P. Li, Exosome: a review of its classification, isolation techniques, storage, diagnostic and targeted therapy applications, Int. J. Nanomed. 15 (2020) 6917–6934, https://doi.org/10.2147/IJN.S264498.

[17] Y. Tang, Y. Zhou, H.J. Li, Advances in mesenchymal stem cell exosomes: a review, Stem Cell Res. Ther. 12 (2021) 71, https://doi.org/10.1186/s13287-021-02138-7.

[18] H. Qiu, S. Liu, K. Wu, R. Zhao, L. Cao, H. Wang, Prospective application of exosomes derived from adipose-derived stem cells in skin wound healing: a review, J. Cosmet. Dermatol. 19 (2020) 574–581, https://doi.org/10.1111/jocd.13215.

[19] I. Kimiz-Gebologlu, S.S. Oncel, Exosomes: large-scale production, isolation, drug loading efficiency, and biodistribution and uptake, J. Contr. Release 347 (2022) 533–543, https://doi.org/10.1016/j.jconrel.2022.05.027.

[20] K. Yue, S.G. Trujillo-de, M.M. Alvarez, A. Tamayol, N. Annabi, A. Khademhosseini, Synthesis, properties, and biomedical applications of gelatin methacryloyl (GelMA) hydrogels, Biomaterials 73 (2015) 254–271, https://doi.org/10.1016/j.biomaterials.2015.08.045.

[21] S. Xiao, T. Zhao, J. Wang, C. Wang, J. Du, L. Ying, et al., Gelatin methacrylate (GelMA)-Based hydrogels for cell transplantation: an effective strategy for tissue engineering, Stem Cell Rev Rep 15 (2019) 664–679, https://doi.org/10.1007/s12015-019-09893-4.

[22] A.G. Kurian, R.K. Singh, K.D. Patel, J.H. Lee, H.W. Kim, Multifunctional GelMA platforms with nanomaterials for advanced tissue therapeutics, Bioact. Mater. 8 (2022) 267–295, https://doi.org/10.1016/j.bioactmat.2021.06.027.

[23] M. Sun, X. Sun, Z. Wang, S. Guo, G. Yu, H. Yang, Synthesis and properties of gelatin methacryloyl (GelMA) hydrogels and their recent applications in load-bearing tissue, Polymers 10 (2018), https://doi.org/10.3390/polym10111290.

[24] I. Pepelanova, K. Kruppa, T. Scheper, A. Lavrentieva, Gelatin-Methacryloyl (GelMA) hydrogels with defined degree of functionalization as a versatile toolkit for 3D cell culture and extrusion bioprinting, Bioengineering (Basel) 5 (2018), https://doi.org/10.3390/bioengineering5030055.

[25] S. Ansari, S.S. Pouraghaei, C. Chen, P. Sarrion, A. Moshaverinia, RGD-modified alginate-GelMA hydrogel sheet containing gingival mesenchymal stem cells: a unique platform for wound healing and soft tissue regeneration, ACS Biomater. Sci. Eng. 7 (2021) 3774–3782, https://doi.org/10.1021/acsbiomaterials.0c01571.

[26] S. Xiao, T. Zhao, J. Wang, C. Wang, J. Du, L. Ying, et al., Gelatin methacrylate (GelMA)-Based hydrogels for cell transplantation: an effective strategy for tissue engineering, Stem Cell Rev Rep 15 (2019) 664–679, https://doi.org/10.1007/s12015-019-09893-4.

[27] F. Ghorbani, L. Moradi, M.B. Shadmehr, S. Bonakdar, A. Droodinia, F. Safshekan, In-vivo characterization of a 3D hybrid scaffold based on PCL/decellularized aorta for tracheal tissue engineering, Mater Sci Eng C Mater Biol Appl 81 (2017) 74–83, https://doi.org/10.1016/j.msec.2017.04.150.

[28] F. Sun, Y. Lu, Z. Wang, B. Zhang, Z. Shen, L. Yuan, et al., Directly construct microvascularization of tissue engineering trachea in orthotopic transplantation, Mater Sci Eng C Mater Biol Appl 128 (2021), 112201, https://doi.org/10.1016/j.msec.2021.112201.

[29] B. Zhang, F. Sun, Y. Lu, Z. Wang, Z. Shen, L. Yuan, et al., A novel decellularized trachea preparation method for the rapid construction of a functional tissue engineered trachea to repair tracheal defects, J. Mater. Chem. B 10 (2022) 4810–4822, https://doi.org/10.1039/d1tb02100a.

[30] F. Sun, S. Pan, H.C. Shi, F.B. Zhang, W.D. Zhang, G. Ye, et al., Structural integrity, immunogenicity and biomechanical evaluation of rabbit decelluarized tracheal matrix, J. Biomed. Mater. Res. 103 (2015) 1509–1519, https://doi.org/10.1002/jbm.a.35273.

[31] F. Sun, Y. Lu, Z. Wang, B. Zhang, Z. Shen, L. Yuan, et al., Directly construct microvascularization of tissue engineering trachea in orthotopic transplantation, Mater Sci Eng C Mater Biol Appl 128 (2021), 112201, https://doi.org/10.1016/j.msec.2021.112201.

[32] S. Pan, Y. Zhong, Y. Shan, X. Liu, Y. Xiao, H. Shi, Selection of the optimum 3D-printed pore and the surface modification techniques for tissue engineering tracheal scaffold in vivo reconstruction, J. Biomed. Mater. Res. 107 (2019) 360–370, https://doi.org/10.1002/jbm.a.36536.

[33] D. Taniguchi, K. Matsumoto, T. Tsuchiya, R. Machino, Y. Takeoka, A. Elgalad, et al., Scaffold-free trachea regeneration by tissue engineering with bio-3D printing, Interact. Cardiovasc. Thorac. Surg. 26 (2018) 745–752, https://doi.org/10.1093/icvts/ivx444.

[34] J.E. Dennis, K.G. Bernardi, T.J. Kean, N.E. Liou, T.K. Meyer, Tissue engineering of a composite trachea construct using autologous rabbit chondrocytes, J Tissue Eng Regen Med 12 (2018) e1383–e1391, https://doi.org/10.1002/term.2523.

[35] E.M. Boazak, D.T. Auguste, Trachea mechanics for tissue engineering design, ACS Biomater. Sci. Eng. 4 (2018) 1272–1284, https://doi.org/10.1021/acsbiomaterials.7b00738.

[36] Y. Xu, E.J. Gao, L. Duan, G.N. Jiang, Research progress of circumferential tracheal reconstruction via tissue-engineered trachea, Zhonghua Wai Ke Za Zhi 60 (2022) 104–109, https://doi.org/10.3760/cma.j.cn112139-20210206-00073.

[37] F. Sun, Y. Lu, Z. Wang, H. Shi, Vascularization strategies for tissue engineering for tracheal reconstruction, Regen. Med. 16 (2021) 549–566, https://doi.org/10.2217/rme-2020-0091.

[38] K. Rashid, A. Ahmad, S.S. Meerasa, A.Q. Khan, X. Wu, L. Liang, et al., Cancer stem cell-derived exosome-induced metastatic cancer: an orchestra within the tumor microenvironment, Biochimie 212 (2023) 1–11, https://doi.org/10.1016/j.biochi.2023.03.014.

[39] R. Wu, H. Li, C. Sun, J. Liu, D. Chen, H. Yu, et al., Exosome-based strategy for degenerative disease in orthopedics: recent progress and perspectives, J Orthop Translat 36 (2022) 8–17, https://doi.org/10.1016/j.jot.2022.05.009.

[40] M.I. Nasser, M. Masood, S. Adlat, D. Gang, S. Zhu, G. Li, et al., Mesenchymal stem cell-derived exosome microRNA as therapy for cardiac ischemic injury, Biomed. Pharmacother. 143 (2021), 112118, https://doi.org/10.1016/j.biopha.2021.112118.

[41] J. Ding, X. Wang, B. Chen, J. Zhang, J. Xu, Exosomes derived from human bone marrow mesenchymal stem cells stimulated by deferoxamine accelerate cutaneous wound healing by promoting angiogenesis, BioMed Res. Int. 2019 (2019), 9742765, https://doi.org/10.1155/2019/9742765.